Running Pulses of Complex Shape in a Reaction-Diffusion Model

E. S. Lobanova[1] and F. I. Ataullakhanov[1,2,3]

[1]*National Research Center for Hematology, Russian Academy of Medical Sciences, Moscow, Russia*
[2]*Physics Department, Moscow State University, Moscow, Russia*
[3]*Institute of the Theoretical and Experimental Biophysics, Pushchino, Moscow Region, Russia*

(Received 1 June 2004; published 26 August 2004)

In a one-dimensional reaction-diffusion model of an active medium, stable steady-state wave pulses of a new type are described. They are called multihumped because their waveforms contain several maxima of similar size. Presumably, the multihumped pulses arise via a bifurcation at which an unstable trigger wave disappears. The parameter governing this bifurcation is the diffusion coefficient for the model inhibitor. The model is analyzed by varying this parameter to determine the conditions for the emergence of multihumped pulses. The results of this analysis show how their waveform and dynamics of excitation depend on the inhibitor diffusion coefficient.

DOI: 10.1103/PhysRevLett.93.098303 PACS numbers: 82.40.Bj, 87.19.Tt

Localized pulses propagating without shape change and at a constant speed are well-known wave solutions to many models of excitable media. Their waveforms can be simple, with one extremum, or complex, with several extrema (spatial oscillations). Spatially localized wave solutions of complex shape are described, for example, in a two-component piecewise linear FitzHugh-Nagumo model with one spatially uniform state and have spatial oscillations in waveforms around the spatially uniform state [1]. Such solutions either are solitary pulses, with the waveform consisting of one large maximum and small-amplitude damped oscillations superimposed on its tail portion, or have waveforms with several large maxima alternating with small-amplitude oscillations. Complex running pulses of yet another type are observed in a two-component model of CO oxidation on Pt with three spatially uniform states [2]. Specifically, extended pulses are described, with most of their waveform being spatial damped oscillations around upper or middle spatially uniform states.

In this study, one more type of running pulses of complex shape (Fig. 1) is reported that we have revealed in the three-component reaction-diffusion model of blood clotting (BC model) with three spatially uniform states (1). Complex pulses in the BC model have spatial oscillations in most of their waveform around the upper spatially uniform state. Spatial oscillations are similar in amplitude, and the number of spatial oscillations can be large. They also differ from the complex pulses in the FitzHugh-Nagumo model and the model of CO oxidation on Pt in that BC model pulses with a large number of spatial oscillations are stable. For their specific appearance, we call these solutions multihumped pulses. Pulses of a complex shape in the model of blood clotting may be of particular interest because they arise via a bifurcation at which an unstable trigger wave disappears.

BC model.—Model (1) of an excitable medium was developed previously [3] to describe the spatial dynamics of blood clotting.

$$\begin{cases} \frac{\partial u_1}{\partial t} = D_a \frac{\partial^2 u_1}{\partial x^2} + K_1 u_1 u_2 (1 - u_1) \frac{(1+K_2 u_1)}{(1+K_3 u_3)} - u_1, \\ \frac{\partial u_2}{\partial t} = D_c \frac{\partial^2 u_2}{\partial x^2} + u_1 - K_4 u_2, \\ \frac{\partial u_3}{\partial t} = D_i \frac{\partial^2 u_3}{\partial x^2} + K_5 u_1^2 - K_6 u_3. \end{cases} \quad (1)$$

The variables of this model are activator (u_1), inhibitor (u_3), and catalyst (u_2) concentrations. Six constants, K_1 through K_6, which are combinations of the rate constants for individual reactions of the clotting cascade, were set to the following values: $K_1 = 6.85$, $K_2 = 7.0$, $K_3 = 2.36$, $K_4 = 0.1$, $K_5 = 14.0$, and $K_6 = 0.08$. In previous studies [3,4], the diffusion coefficients for activator, inhibitor, and catalyst were assumed to be equal: $D_a = D_c = D_i$. Multihumped pulses are observed in the model upon decreasing the inhibitor diffusion coefficient. Therefore, analyzing model behavior, we varied its value from 1 to 0, while keeping the other two diffusion coefficients fixed ($D_a = D_c = 1$). The main results of this analysis are presented in this study. Near its critical values, the bifurcation parameter is varied in decrements of 0.001.

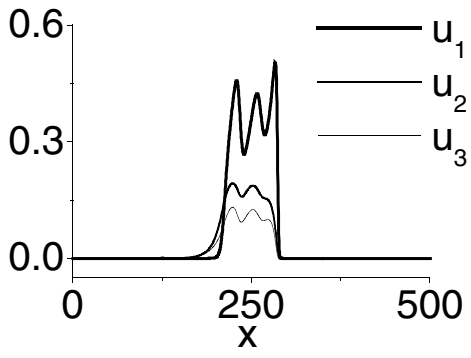

FIG. 1. A pulse of complex shape, with the catalyst (u_2) and inhibitor (u_3) concentrations brought to the scale by normalizing them by factors of 20 and 200, respectively.

To analyze the dynamic modes, we solve Eqs. (1), using a simple explicit difference scheme and the no-flux boundary conditions. The space step h is 0.25; the time step τ is 0.01. The model has a trivial stable spatially uniform steady-state solution with threshold properties. The initial conditions were chosen in the form of a local rise in the activator concentration above the threshold value at the left end of the segment.

The steady-state solutions corresponding to the waves, which travel at a constant speed without changes in waveform, are also obtained by numerically solving the nonlinear ordinary differential Eqs. (2) derived from Eqs. (1) for the coordinate system moving with velocity c. This approach allows one to obtain both stable and unstable solutions. To test a solution for stability, we slightly perturb it and take it as the initial conditions for solving Eqs. (1). During computations, unstable solutions decay. In Eqs. (2), the prime denotes a derivative with respect to the coordinate in the coordinate system where the wave is standing.

$$\begin{cases} D_a \nu_1'' + c\nu_1' + K_1\nu_1\nu_2(1-\nu_1)\frac{(1+K_2\nu_1)}{(1+K_3\nu_3)} - \nu_1 = 0, \\ D_c \nu_2'' + c\nu_2' + \nu_1 - K_4\nu_2 = 0, \\ D_i \nu_3'' + c\nu_3' + K_5\nu_1^2 - K_6\nu_3 = 0, \\ \nu_1'(0) = \nu_2'(0) = \nu_3'(0) = \nu_1'(L) = \nu_2'(L) = \nu_3'(L) = 0. \end{cases} \quad (2)$$

At the chosen values of parameters K_1–K_6, multihumped pulses are observed in the model if the inhibitor diffusion coefficient D_i is smaller than some critical value: $D_i < D_i^{cr}$ ($D_i^{cr} \sim 0.703$). If $D_i^{cr} < D_i \leq 1$, intricate dynamic regimes set in by unstable trigger waves that bring the medium from its lower (trivial) stable steady state to the upper (nontrivial) unstable steady state. We believe that it is a bifurcation of these waves that gives rise to multihumped pulses. Therefore, we decrease the diffusion coefficient for the inhibitor below unity and describe how the model regimes change with its decrease.

Trigger waves are steady-state wave solutions to reaction-diffusion models. They propagate at a constant speed without changing in shape and switch the medium between its two spatially uniform states [5]. Stable trigger waves usually exist in the regions of parameter space where the respective model without spatial variables (homogeneous model) is bistable. In these regions, the model with spatial variables has two coexisting stable spatially uniform states (we call them lower and upper) and one unstable state between them. On varying the parameters, the upper state can lose stability but continue to exist. As a result, we often observed that the model not only had the spatially uniform stable state, but also retained the solution in the form of a trigger wave that brought the medium from the lower stable state to the upper, already unstable state. Obviously, such trigger waves are unstable. However, their effect on the dynamic behavior of the Gray-Scott model [6], the model of CO oxidation on Pt [7], the FitzHugh-Nagumo model with modified nonlinearity [8], and the model of blood clotting [4] is significant: chaotic or nonstationary modes are generated whose spatiotemporal patterns contain the front portions of these unstable trigger waves.

At the chosen values of parameters K_1–K_6 and the inhibitor diffusion coefficient D_i in the range $D_i^{cr} < D_i \leq 1$, nonstationary modes generated by unstable trigger waves are observed in the BC model [9]. Figure 2(a) shows a mode developing in response to activation at $D_i = 1$. Excitation spreading from the site of activation at the left end of the segment sets the oscillation regime over the entire segment. In the front portion of excitation, one can distinguish a leading edge, which looks like a trigger wave. It runs at a constant speed and does not vary in shape. Both its shape and speed closely coincide with the respective characteristics of the unstable trigger wave calculated at these parameter values from the solution to Eqs. (2) [Fig. 3(a), $D_i = 1$]. The rear part of the leading wave oscillates and generates pulses that fill up all the space behind the wave. These pulses tend to form waves whose fronts also resemble the fronts of unstable trigger waves. The latter fact is easy to see if we, for example, set all the three variables over most of the segment to zero, leaving just one pulse behind the leading wave, and then continue computations. Eventually, waves of the same kind develop from this pulse [see Fig. 2(a); cf. $t = 1800$, a single pulse extracted from panel $t = 1800$, and $t = 2000$].

As long as the diffusion coefficient for the inhibitor remains larger than its critical value ($D_i > D_i^{cr}$), unstable trigger waves generate dynamic modes of the type described above. With D_i decreasing to D_i^{cr}, the waveform of unstable trigger waves changes: the number of spatial oscillations around the upper state increases [Fig. 3(a)]. The dynamic regimes generated by these waves also change as D_i approaches D_i^{cr}; they contain waves with more and more oscillations around the upper state in their front portion [cf. Fig. 3(a) with the dynamic modes shown in Figs. 2(a)–2(d)]. When D_i is set to its critical value ($\sim$0.703), no trigger wave exists any longer.

A further decrease in the diffusion coefficient for the inhibitor below its critical value ($D_i < D_i^{cr}$) alters the model behavior, and pulses of complex shapes become components of spatiotemporal patterns [9]. Figure 2(e) shows a regime obtained in response to activation for $D_i = 0.702$, i.e., D_i only slightly smaller than D_i^{cr}. The zone of nonstationary regimes begins to expand from the site of activation. In the front part of this zone, an extended pulse is gradually formed, with the waveform containing many spatial oscillations. Behind this pulse, oscillations continually varying in shape and spatial period are observed. At smaller D_i, the regimes generated by activation contain localized waves with the waveform containing spatial oscillations, but their number

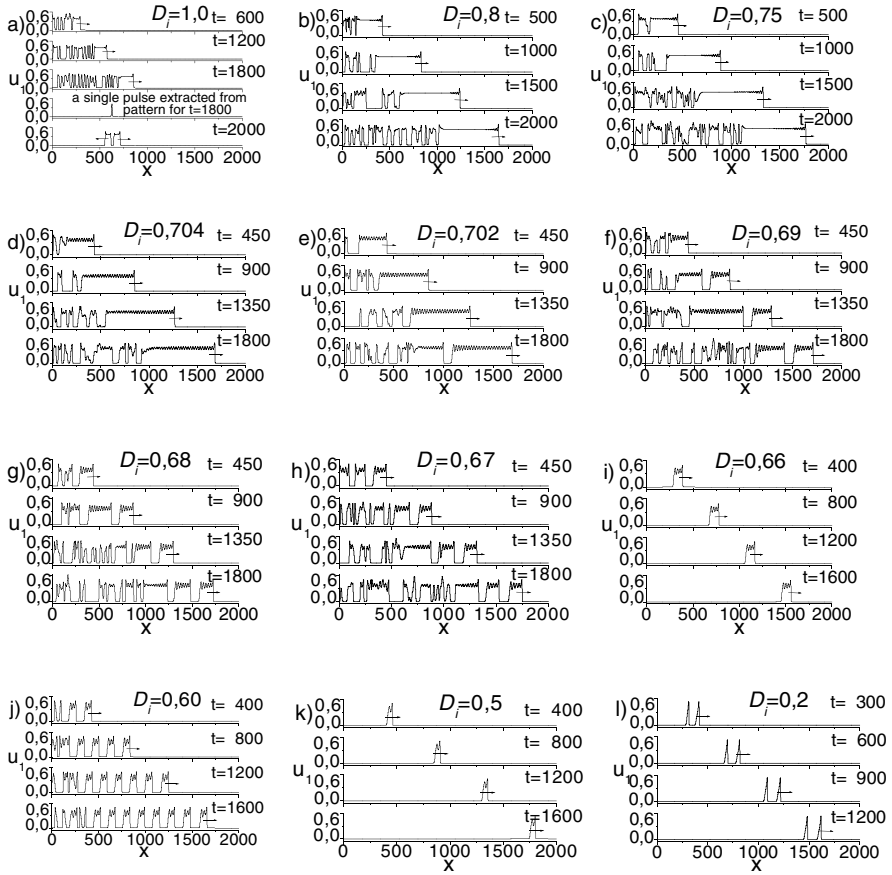

FIG. 2. Dynamic regimes excited in the BC model by activation at the left end of the segment computed for D_i of (a) 1.0, (b) 0.80, (c) 0.75, (d) 0.704, (e) 0.702, (f) 0.69, (g) 0.68, (h) 0.67, (i) 0.66, (j) 0.60, (k) 0.50, and (l) 0.20. For each curve, the time to which it corresponds is shown at the right. Dynamic regimes are excited by an increase of activator concentration ($u_1 = 0.2$) in 80 nodes at the left end of the segment.

progressively decreases [Figs. 2(e)–2(l)]. Eventually, at small D_i values, the solutions become simple pulses [Fig. 2(l)].

Several scenarios can be distinguished whereby multihumped pulses are excited in response to activation. In one case, one or more pulses of complex shape arise ahead of the zone of continually varying modes expanding from the site of activation [Figs. 2(e)–2(h)]. In yet another case, a solitary pulse of complex shape is formed [Figs. 2(i) and 2(k)]. In a third case, a zone of oscillations arises at some distance away from the site of activation and generates identical single pulses of complex shape [Fig. 2(j)]. At values of the diffusion coefficient for inhibitor considerably below unity, two simple pulses are formed, one lagging behind the other [Fig. 2(l)].

To ensure that the pulses of complex shape are steady-state solutions to the model, we took values of all variables along the segment and identified single well-developed multihumped pulses [Figs. 2(e)–2(l)]. We estimated their speed c and used this estimate as the initial conditions for solving the nonlinear boundary-value problem. These computations confirmed that pulses of complex shape are solutions to Eqs. (2) and, as such, are steady-state solutions to Eqs. (1). Figure 3(b) shows the waveforms of complex pulses of activator for different values of the inhibitor diffusion coefficient. The distinctive features of these pulses are that the amplitude and frequency of the spatial oscillations in their waveform vary little with the diffusion coefficient and that the spatial oscillations are around the unstable upper spatially homogeneous state (indicated by a horizontal dashed line). The smaller the diffusion coefficient, the smaller the number of spatial oscillations (humps) in the pulse waveforms.

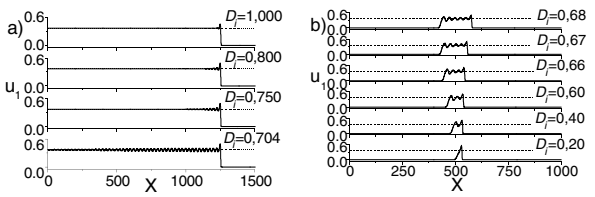

FIG. 3. (a) Unstable trigger waves and (b) solitary multihumped pulses at different inhibitor diffusion coefficients.

Discussion.—In a broad parameter range, the BC model has in addition to a trivial (lower) stable spatially homogeneous state a nontrivial solution in the form of an unstable trigger wave that brings the medium from the stable lower state to the unstable upper state. At these parameters solving the partial differential equations of the model, one observes the spatiotemporal patterns of nonstationary modes that contain the front portions of these unstable trigger waves. A decrease in the diffusion coefficient for the inhibitor below some critical value D_i^{cr} results in the unstable trigger wave disappearing while the stable complex pulses (with spatial oscillations in their waveforms) emerge. Moreover, the fact that the trigger wave contains more and more spatial oscillations around the upper state in the waveform as the parameter approaches its critical value from above, as well as the presence of similar oscillations around the upper state in the waveforms of multihumped pulses at the parameter values smaller than the critical one, lead us to speculate that multihumped pulses arise directly from the trigger wave.

Yet another argument in favor of multihumped pulses originating from trigger waves comes from comparative analysis of the steady-state waveforms of the wave solutions (trigger waves and multihumped pulses) to model (1) in the (u_1, u_2, u_3) space.

Unstable trigger waves in the (u_1, u_2, u_3) space are lines connecting the points corresponding to the lower and upper spatially homogeneous states of the model [Figs. 4(a)–4(c)]. With a reduction in the inhibitor diffusion coefficient, spatial oscillations in the waveforms of unstable trigger waves increase in number. In the (u_1, u_2, u_3) space, trigger waves with oscillations around the upper state are first monotonic curves when they leave the lower state; before reaching the upper point, they perform several intertwining turns around the upper state. The closer the diffusion coefficient for the inhibitor is to its critical value, the more turns around the upper state the trajectory performs before it enters the upper point [cf. Figs. 4(b) and 4(c)].

At $D_i < D_i^{cr}$, the model has a solution in the form of multihumped pulses, which appear in the (u_1, u_2, u_3) space as lines running monotonically when they come out of the lower state toward the upper one; after several untwisted turns around the upper state, they return to the lower state [Figs. 4(d) and 4(e)]. Each turn around the upper state corresponds to one hump in the running pulse. The smaller the diffusion coefficient for the inhibitor, the fewer turns around the upper state are in the trajectory before it returns to the lower point [cf. Figs. 4(d) and 4(e)].

Running pulses of complex shape detected in the BC model broaden the range of possible bifurcations of trigger waves. It is not unexpected if pulses of complex shape would be detected in other reaction-diffusion models that have solutions in the form of unstable trigger waves. The likely bifurcation parameters for the emergence of such pulses are those whose change causes the number of spatial oscillations around the unstable spatially homogeneous states of the models in their waveform to vary.

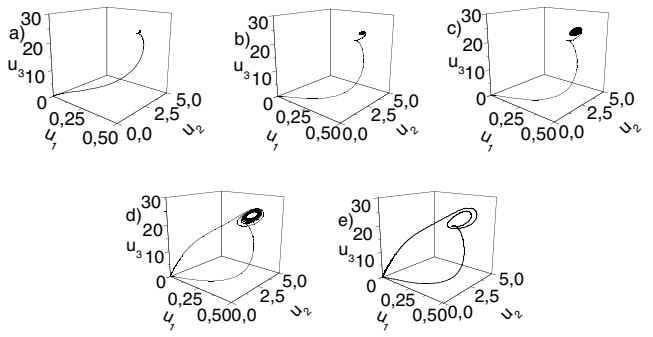

FIG. 4. Unstable trigger waves and solitary multihumped pulses in (u_1, u_2, u_3) space computed for D_i of (a) 1, (b) 0.75, (c) 0.704, (d) 0.702, and (e) 0.6.

This work was supported by the Russian Foundation for Basic Research, Project No. 03-04-48 338. The authors are grateful to Professor E. E. Shnol for discussions of this work.

[1] Yu. A. Kuznetsov, *Elements of Applied Bifurcation Theory* (New York, Springer, 1998).
[2] J. Krishnan, I. G. Kevrekidis, M. Or-Guil, M. G. Zimmermann, and M. Bar, Comput. Methods Appl. Mech. Eng. **170**, 253 (1999).
[3] V. I. Zarnitsina, F. I. Ataullakhanov, A. I. Lobanov, and O. L. Morozova, Chaos **11**, 57 (2001).
[4] E. S. Lobanova and F. I. Ataullakhanov, Phys. Rev. Lett. **91**, 138301 (2003).
[5] A. Hagberg and E. Meron, Nonlinearity **7**, 805 (1994).
[6] J. H. Merkin, V. Petrov, S. K. Scott, and K. Showalter, Phys. Rev. Lett. **76**, 546 (1996).
[7] M. G. Zimmermann *et al.*, Physica (Amsterdam) **110D**, 92 (1997).
[8] V. B. Kazantsev, V. I. Nekorkin, S. Binczak, and J. M. Bilbault, Phys. Rev. E **68**, 017201 (2003).
[9] See EPAPS Document No. E-PRLTAO-93-092434 for video files showing dynamic regimes and multihumped pulses presented in Figs. 2(a)–2(l). A direct link to this document may be found in the online article's HTML reference section. The document may also be reached via the EPAPS homepage (http://www.aip.org/pubservs/epaps.html) or from ftp.aip.org in the directory /epaps/. See the EPAPS homepage for more information.